

Determination of Naturally Occurring Radionuclides Concentration in Environmental Samples in West Kirby Area Using Gamma-Ray Spectroscopy

Ekundayo Oki Akinduro¹

¹ Radiometrics, School of Physical Sciences, University of Liverpool, United Kingdom

Correspondence: Ekundayo Akinduro, Department of Physics, Coleg Cambria, Grove Park, Wrexham, LL12 7AB, United Kingdom.

Received: August 3, 2022

Accepted: September 5, 2022

Online Published: October 27, 2022

doi:10.5539/mas.v16n4p40

URL: <https://doi.org/10.5539/mas.v16n4p40>

Abstract

The purpose of this work is to investigate and evaluate the level of contamination of naturally occurring radionuclides in environmental soil samples collected at a place from West Kirby using gamma-ray spectroscopy. The Broad Energy Germanium (BEGe2825) detector has the ability to detect gamma-rays in the range of 3 keV-3MeV. This detector offers a very good resolution, low noise performance and almost ideal Gaussian shape in our analysis. Under our depth of interest of 0 – 48 cm, a total of six spectra were measured. From known values of gamma-ray energies, a calibrated curve was plotted. From the analysis, the mean activity concentration of naturally radionuclides of uranium-238, thorium-232 and potassium-40 obtained are 6.7 ± 0.1 Bq/kg, 5.6 ± 0.1 Bq/kg and 398.2 ± 8.2 Bq/kg were found in the range of $(5.37 \pm 0.30 - 8.86 \pm 0.40)$ Bq/kg, $(4.37 \pm 0.31 - 8.72 \pm 0.35)$ Bq/kg and $(384 \pm 19 \text{ and } 416 \pm 21)$ Bq/kg respectively. Man-made radionuclides of americium-241 and cesium-137 mean activity concentrations are 4.3 ± 0.1 Bq/kg and 14.5 ± 0.3 Bq/kg were found in the range of (BDL: 5.95 ± 0.32) Bq/kg and $(6.66 \pm 0.35 - 29.2 \pm 1.5)$ Bq/kg respectively.

Keywords: radioactivity concentrations, activity, BEGe gamma spectrometry, U-238, Th-232, Am-241, Cs-137, K-40

1. Introduction

The discovery of radioactivity from uranium-bearing rock in 1896 by Becquerel has opened the pace for detailed and intensive studies. Notable scientist like Marie and Pierre Curie and Ernest Rutherford have studied and revealed the true nature of radioactive (Lilley, 2001). The studying of radioactivity phenomena, its application and effects to human being, environment and existence is still going on. It was discovered that radioactivity occurs due the decay of unstable radioactive nuclides. In an attempt for this unstable nuclide to become stable, it releases energy and matter in the form of radiation. The three-main radiation emitted by radioactive materials are alpha, beta and gamma radiation (Knoll, 2010). Radioactivity can be natural or man-made. Some of the radioactive nuclides are found in nature throughout the environment in soil, food, water and atmosphere which clearly proved that we interact with radioactivity as part of our lives daily (Kathren, 1998). In order to determine the extent of pollution of natural radionuclides in our life and environment has brought about many different techniques to identify clearly and quantify the radionuclides present (Abu-Haija, 2012). The most efficient used method is gamma-ray spectroscopy.

Gamma-ray spectroscopy is a basic analytical method in the nuclear technology clear identification and effective quantification of radionuclides present in soil, sediments or a various mixture of isotopes. This method is based on the detection of gamma ray emission from a radioactive source during its unstable decay. Gamma ray having the highest energy among all the electromagnetic radiation make it easy for the gamma-ray spectrometer to measure and display the energies of detected gamma -ray photons. The gamma-radiation is released as the excited state de-excited to the ground state (Gilmore & Heamingway, 2008).

The measured energy corresponds to a photo-peak of the spectrum of the element in a sample and its isotopes that is gamma photon energy is a characteristic of a nuclide. Its counts rate gives its abundance that is why gamma ray spectroscopy has the ability to effectively determine both counts rate and the energy emitted from the radioactive source. The use of broad energy germanium (BEGe) detectors has made it possible the correlation of

the photo-peaks from the spectrum and the nuclide characteristic gamma-ray energies. Natural Occurring Radioactive Materials (NORMs) is very important in study radionuclides of uranium-238 series, thorium-232 series and potassium (Barba-Lobo, 2022). This help in the identification of different radionuclides and isotopes present in the sample. The activity levels are low for NORM, the count period need to be long for reasonable statistical results to be obtained (Jones et al., 1989; Lilley, 2001). Gamma-ray Spectroscopy has been put in effective practical applications in environmental studies, monitoring in nuclear facilities, nuclear forensics, health physics, nuclear medicine, identification of clay minerals in petroleum in industrial radioisotopes and so on.

The objective of this work was to investigate the activity concentrations of different naturally occurring radionuclides present between depths 0cm to 48cm at West Kirby of latitude $53^{\circ} 22' 21''$ N and longitude $3^{\circ} 11' 22''$ W.

The radionuclides I expect to detect and quantify its activity concentration in the soil samples are as follow:

- Naturally occurring radionuclides and daughters of uranium-238 series, thorium -232 series and potassium-40 present in the sample soils.
- Anthropogenic radionuclide fission product such as caesium-137 in reprocessing wastes and materials.
- Transuranic nuclide of americium-241, which is recycled uranium and material contaminated by it in the sample soil.

1.1 Location

The investigation of the activity concentrations of different naturally occurring radionuclides present between depths 0cm to 48cm at West Kirby of latitude $53^{\circ} 22' 21''$ N and longitude $3^{\circ} 11' 22''$ W as shown in the map below.

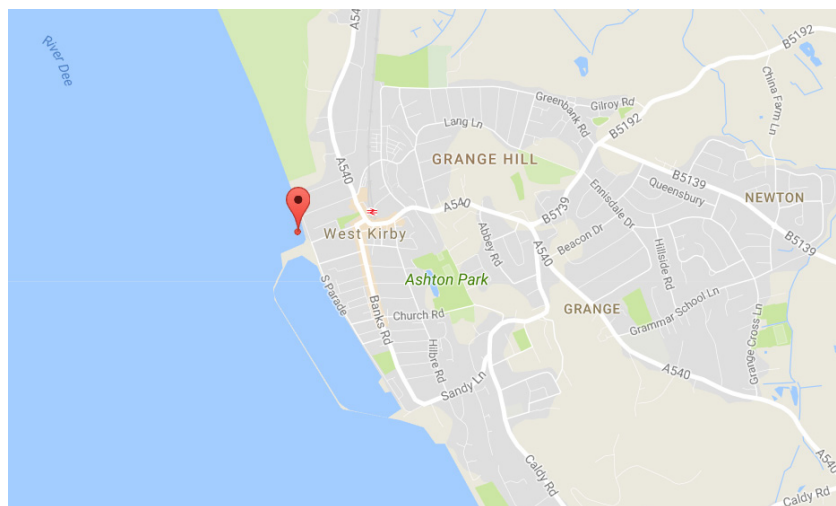


Figure 1A. Google map of the sample location

2. Methods

A sample of six was collected at a depths 0-8cm, 8-16cm, 16-24cm, 24-32cm, 32-40cm and 40-48cm from West Kirby, Liverpool environment of latitude $53^{\circ} 22' 21''$ N and longitude $3^{\circ} 11' 22''$ W. The necessary preparation of large volume pre-concentration and separation for homogeneity and sub-sampling of the samples selected for analysis were done in order to achieve low detection limit.

At Radiation Laboratory, University of Liverpool the sample was dried and then oven drying to driving off moisture in the sediment sample for at least 30 minutes. A specific geometry obtained by crushing samples to fine grains and sieve for homogeneity. Each sample was packed in a 550 ml Marinelli beaker and each weight of the sample with Marinelli beaker measured. The lids were sealed with plastic tape to prevent Rn-220 and Rn-222 from escape and kept for at least thirty days so that secular equilibrium between Ra-226 and Rn-222 reached. It is about 3 months before the running and analysing the samples. The figure 1 below shows prepared soil samples in Marinelli beakers ready for analysis (Knoll, 2010).



Figure 1. Soil samples in 500ml Marinelli beaker

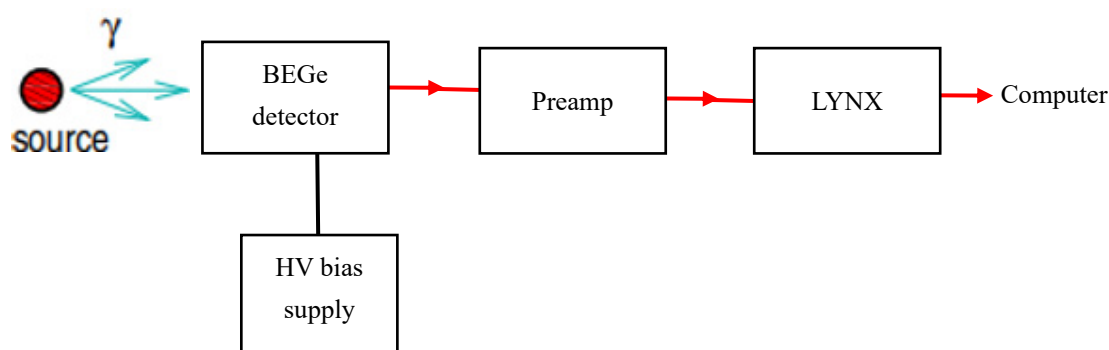


Figure 2. Schematic block diagram of the BEGe detector system

2.1 BEGe Detector System Set-Up

The BEGe detector used for running and analysis of my soil sample was located inside the Radiation laboratory of the University of Liverpool showing the block diagram in figure 2 below. A gamma-ray spectroscopy in this laboratory work composed of a BEGe detector, a pre-amplifier, Lynx, high-voltage power supply, computer and a lead shield. Germanium detectors are preferred to other detectors for the analysis of complex gamma spectra with multi-peaks (Knoll, 2010; Harkness-Brennana et al., 2014).

The photon energies emitted by the radionuclides in the sample detected by the detector for further processing. The BEGe detector was powered by the high bias voltage of 4500 V. The preamplifier converts the current pulse to voltage step proportional to total charge deposited in the detector. The Lynx which is a digital signal analyser digitised the amplitude of the voltage signal delivered as a 14-bit number by the digitizer at a frequency of 80 MHz and shaping time of 12.5 ns. The digital signal analyser used in this work was Lynx of IP: 138.253.96.115. The output was passed to a PC and a software called Prospect was used to create the spectrum of the radionuclides present in the sample (CANBERRA, 2014).

After the BEGe detector has been calibrated and make sure all connection checked and in the correct order. A new empty Marinelli beaker of mass 58.3g and 500ml capacity was placed on the top of the detector. The prospect software set in PHA acquisition mode and run for set live-time of 172800 second due to low activity of background. The spectrum generated over the energy range of interest from 45 keV to 2700 keV.

2.2 Activity Concentration, Detection Limit and Minimum Detectable Activity

2.2.1 Activity Concentration

The activity concentration (Bq/kg), A which the quantification of radioactive nuclides present in a sample can be calculated using equation (1), (Gilmore & Heamingway, 2008).

$$\text{Activity} = \frac{\text{Net count rate}}{\text{Efficiency} \times \text{emission probability} \times \text{sample mass}} \quad (1)$$

Net counts rate = Total Counts rate – Background counts rate.

The uncertainty Activity concentration, ΔA is given as

$$\Delta A = A \times \sqrt{\left(\frac{\Delta E_{ff}}{E_{ff}}\right)^2 + \left(\frac{\Delta N}{N}\right)^2} \quad (2)$$

Where E_{ff} , N , ΔE_{ff} , ΔN are efficiency, Net count rate, uncertain efficiency and uncertainty net count rate respectively.

2.2.2 Critical Limit

In optimising the accuracy of data obtained in gamma-ray spectroscopy it is better to establish its statistical significance. The Critical limit, L_c is defined as the count above which a net signal can reliably be detected. For a confidence level of 95% certain that the count is part of background distribution. The critical limit is calculated using the formula (Gilmore & Heamingway, 2008):

$$L_c = 2.33\sigma_B \quad (3)$$

Where σ_B is the uncertainty of background count equal to $\sqrt{N_B}$ is the standard deviation of the count in the blank sample.

2.2.3 Detectable Limit

The Detection limit, L_D is defined as the minimum expected net count from the sample that can be detected with a significant count. This is taken at a confidence level of 95% certain. The detection can be calculated using the formula (Gilmore & Heamingway, 2008).

$$L_D = 2.71 + 4.65\sigma_B \quad (4)$$

2.2.4 Minimum Detectable Activity

Minimum detectable activity, MDA is defined as the lowest level of activity of a radioactive nuclide in a sample that can be detected with a specified confidence level (Thomas, 1984). MDA depends on the measuring time, the background level and the emission probability. The MDA of gamma-ray measurement for radionuclides of interest were calculated using the equation (5) where sample mass in kg), (Gilmore & Heamingway, 2008).

$$MDA = \frac{\text{Detection Limit}}{\text{Efficiency} \times \text{emission probability} \times \text{Livetime} \times \text{Sample mass}} \quad (5)$$

The uncertainty in MDA was calculated using the equation:

$$\Delta(MDA) = MDA \times \sqrt{\left(\frac{\Delta L_D}{L_D}\right)^2 + \left(\frac{\Delta E_{ff}}{E_{ff}}\right)^2} \quad (6)$$

where L_D , E_{ff} , ΔE_{ff} , ΔL_D are detection limit, detector efficiency, uncertainty in efficiency and uncertainty in detection limit respectively.

3. Background and Samples Measurements

After the BEGe detector has been calibrated and make sure all connection checked and in the correct order. A new empty Marinelli beaker of mass 58.3g and 500ml capacity was placed on the top of the detector. The prospect software set in PHA acquisition mode and run for set live-time of 172800 second due to low activity of background.

The spectrum generated over the energy range of interest from 45 keV to 2700 keV. showing in the spectrum of figures 3, 4, and 5 below.

Table 1. Background measurement, Limit of Detection and MDA

Radio- Nuclide	Energy (KeV)	Net Counts Area	±	Absolute Efficiency	±	Limit of Detection	±	MDA (Bq/kg)	±
Pb-210	46.4	118	79	0.0419	0.0021	53.3	8.9	0.34	0.03
Am-241	59.5	36	92	0.0447	0.0022	30.5	9.6	0.02	0.00
Th-234	63.3	166	63	0.0454	0.0022	62.6	7.9	0.42	0.03
Ac-228	209.1	293	158	0.0399	0.0020	82.3	12.6	0.60	0.05
Pb-212	238.7	3163	113	0.0371	0.0018	264.2	10.6	0.19	0.01
Pb-214	241.5	818	120	0.0368	0.0018	135.7	11.0	0.56	0.03
Ti-208	277.4	865	91	0.0309	0.0015	139.5	9.5	0.78	0.03
Pb-214	295.2	1491	88	0.0317	0.0016	182.3	9.4	0.35	0.01
Pb-212	300.0	318	90	0.0312	0.0014	85.6	9.5	0.95	0.06
Ac-228	338.4	636	69	0.0272	0.0013	120.0	8.3	0.44	0.02
Pb-214	351.9	3136	91	0.0253	0.0013	263.1	9.5	0.31	0.01
Ti-208	583.0	1654	65	0.0181	0.0009	191.8	8.1	0.39	0.01
Bi-214	609.4	3899	81	0.0145	0.0007	293.1	9.0	0.50	0.01
Cs-137	661.7	526	56	0.0126	0.0006	109.4	7.5	0.12	0.00
Bi-212	727.3	553	55	0.0114	0.0006	112.0	7.4	1.67	0.07
Ti-208	860.8	127	35	0.0098	0.0005	55.1	5.9	1.44	0.09
Ac-228	911.4	1531	56	0.0089	0.0004	184.7	7.5	0.91	0.03
Ac-228	969.2	847	48	0.0085	0.0004	138.1	6.9	1.17	0.04
Bi-214	1120.3	1160	54	0.0076	0.0004	161.1	7.3	1.60	0.05
Bi-214	1238.2	529	47	0.0068	0.0003	109.7	6.8	3.18	0.13
K-40	1460.8	1461	97	0.0057	0.0003	180.5	9.9	3.39	0.13
Bi-214	1764.7	1635	47	0.0049	0.0002	190.7	6.9	2.91	0.09

Table 2. Average specific activity levels of U-238, Th-232, K-40, Cs-137 and Am-241 in the samples.

Nuclide	Activity (Bq/kg)	±	Activity (Bq/kg)	±	Activity (Bq/kg)	±	Activity (Bq/kg)	±	Activity (Bq/kg)	±	Activity (Bq/kg)	±
Depth	0-8cm		8-16cm		16-24cm		24-32cm		32-40cm		40-48cm	
U-238	5.37	0.30	6.42	0.36	5.50	0.34	6.38	0.34	6.76	0.35	8.86	0.40
Th-232	5.00	0.33	4.37	0.31	4.40	0.31	5.41	0.33	5.53	0.32	8.72	0.35
Am-241	4.14	0.24	5.95	0.32	5.53	0.30	2.53	0.18	3.47	0.21	BDL	BDL
Cs-137	8.20	0.43	14.95	0.75	19.29	0.97	29.2	1.5	9.01	0.47	6.66	0.35
K-40	384	19	395	20	386	19	416	21	402	20	406	20

*BDL (below detectable limit)

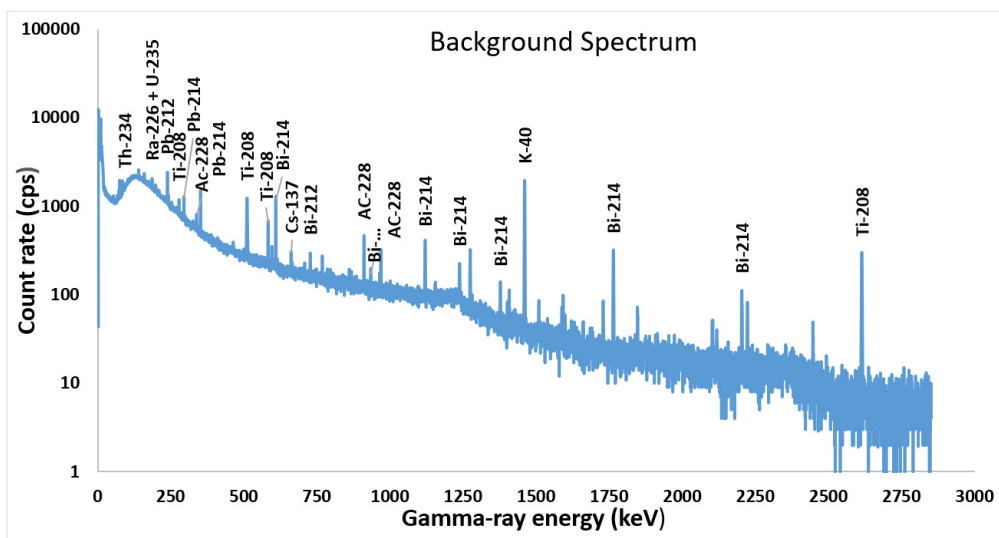


Figure 3. Background spectrum of BEGe detector in the region 1-2875 keV for 172800 s

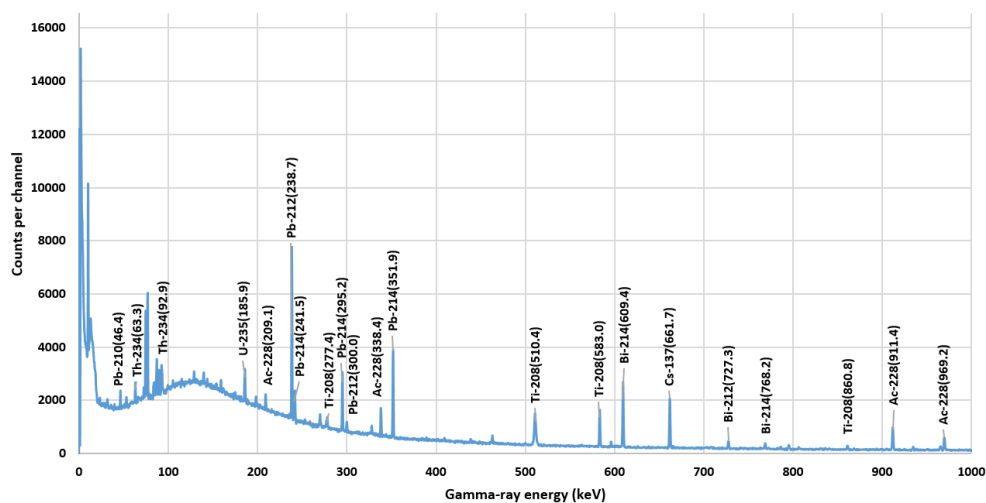


Figure 4. Spectra of the soil at depth 40-48 cm of energy range 0-1000 keV for 172800s

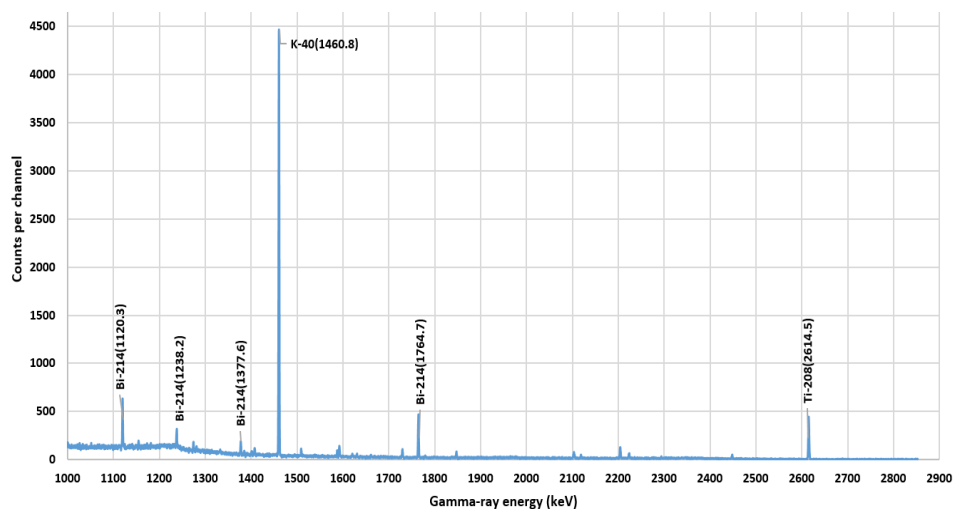


Figure 5. Spectra of soil at depth 40-48 cm of energy range from 1000-2900 keV for 172800s

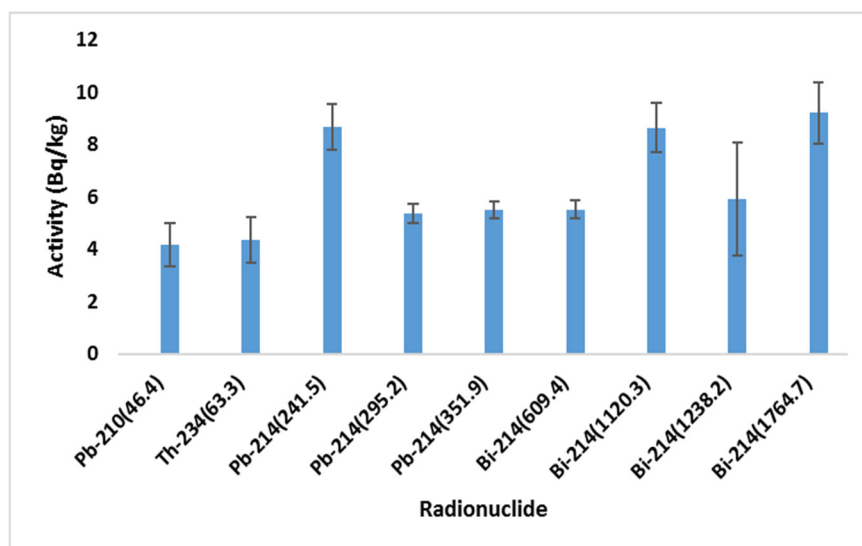


Figure 6. Activity concentration of isotopes in U-238 at soil depth 24-32 cm

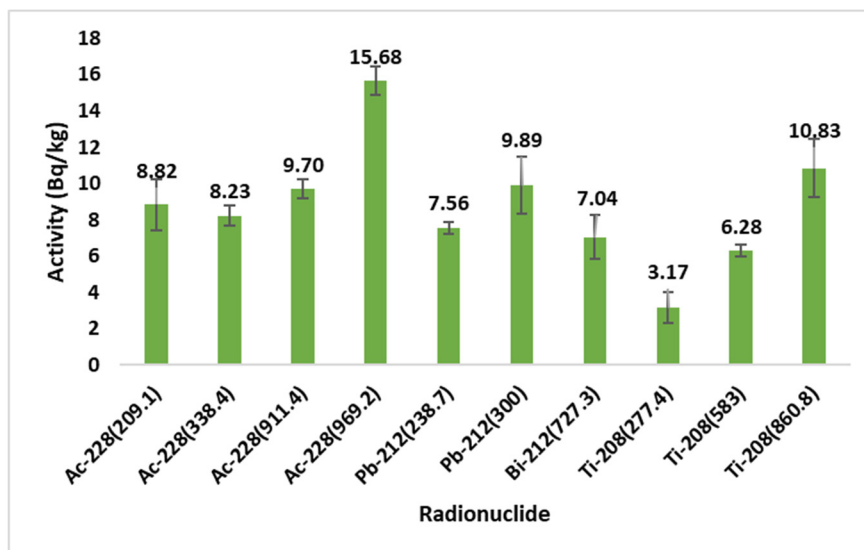


Figure 7. Activity concentration of isotopes in Th-232 at soil depth 24-32 cm

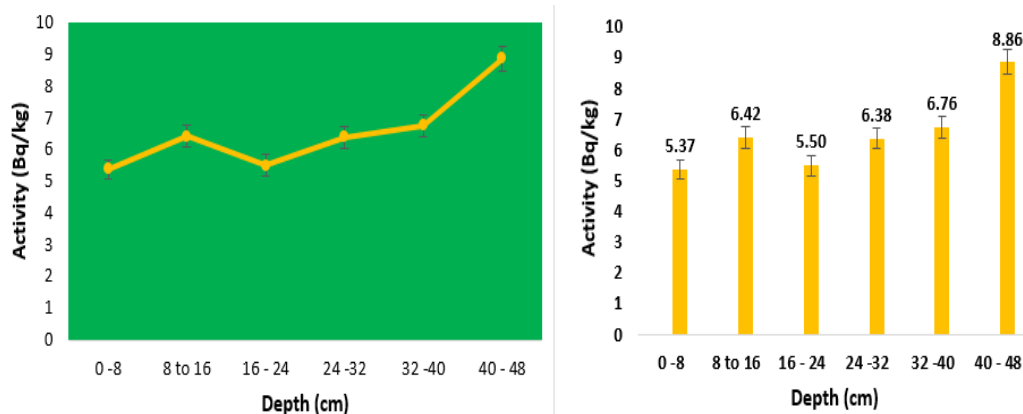


Figure 8. Plots of activity concentration of U-238 at each depth of soil samples

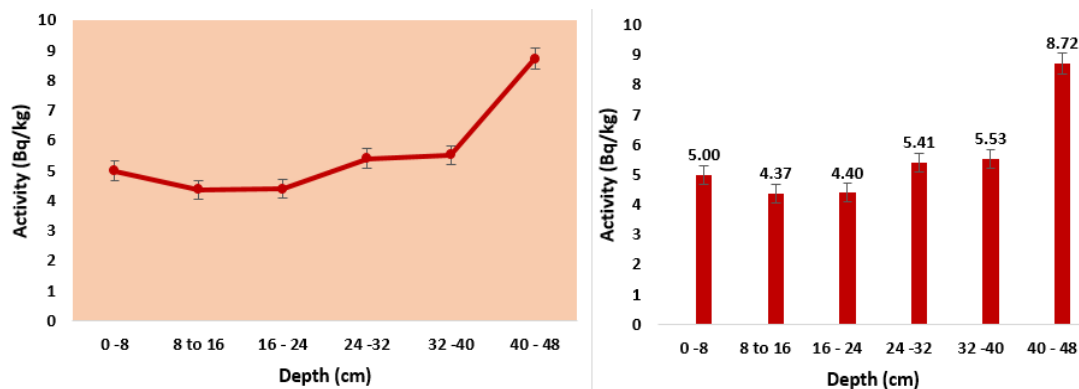


Figure 9. Plots of activity concentration of Th-232 at each depth of soil samples

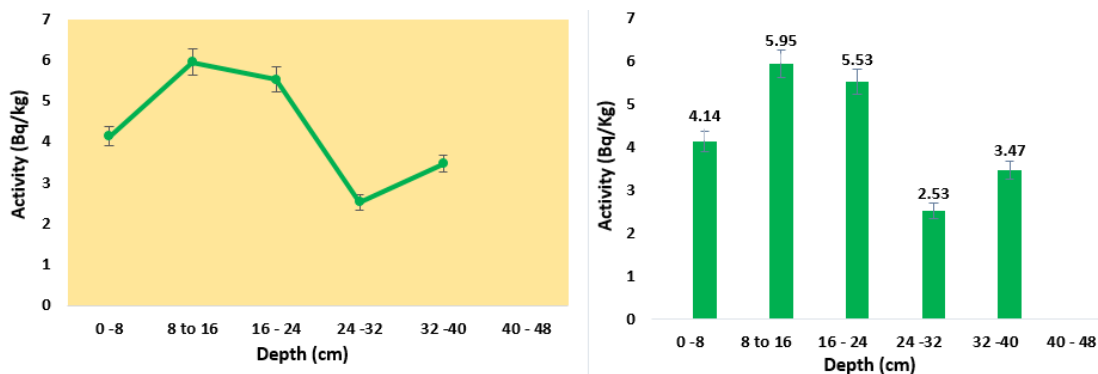


Figure 10. Plots of activity concentration of Am-241 at each depth of soil samples

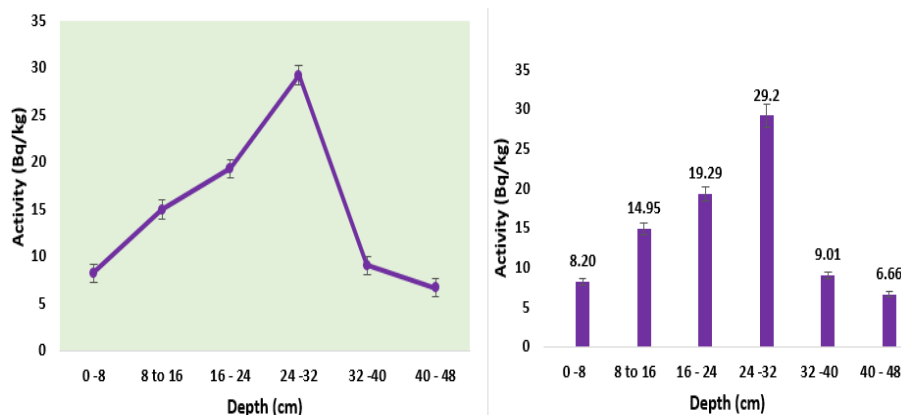


Figure 11. Plots of activity concentration of Cs-137 at each depth of soil samples

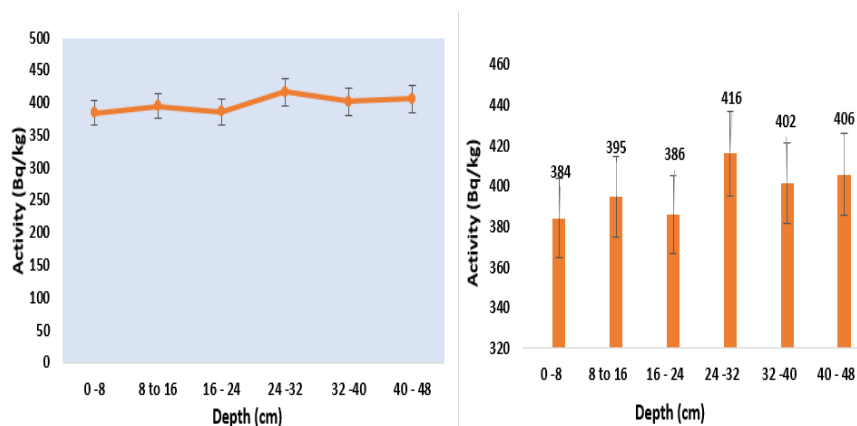


Figure 12. Plots of activity concentration of K-40 at each depth of soil samples

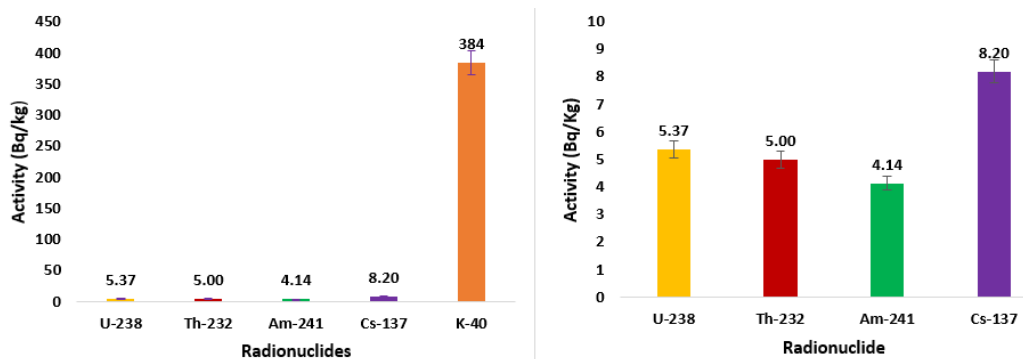


Figure 13a. Activity conc. of radionuclides at depth 0-8 cm with K-40

Figure 13b. Activity conc. at depth 0-8 cm without K-40

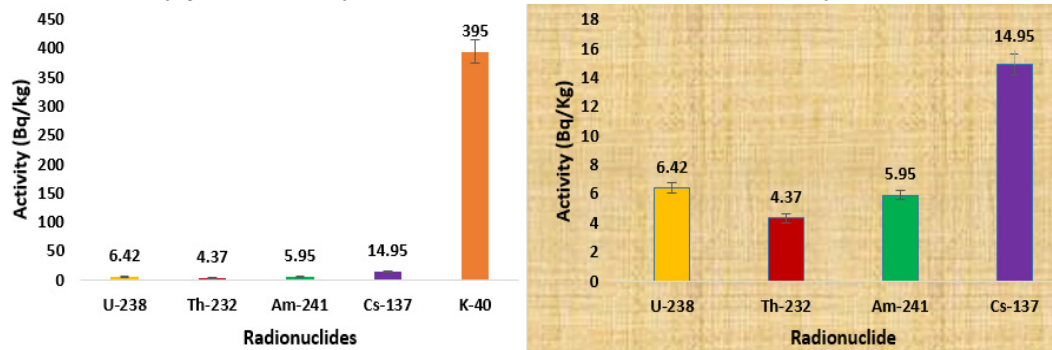


Figure 14a. Activity conc. at depth 8-16 cm with K-40

Figure 14b. Activity conc. at depth 8-16 cm without K-40

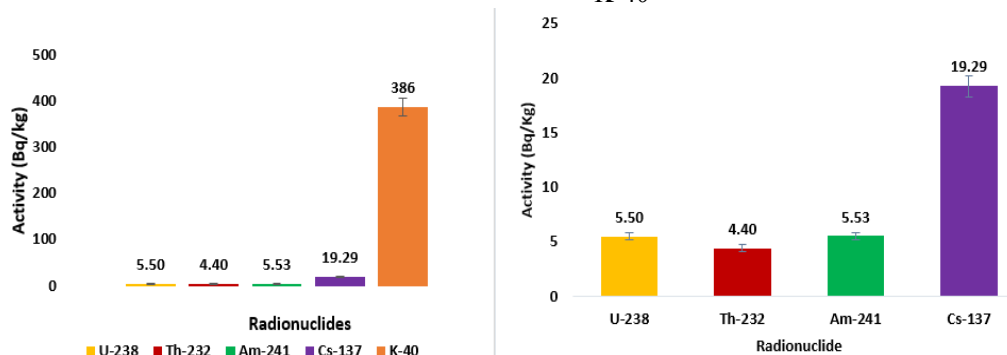


Figure 15a. Activity conc. at depth 16-24 cm with K-40

Figure 15b. Activity conc. at depth 16-24 cm without K-40

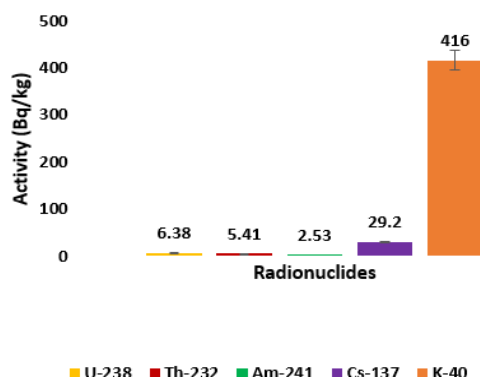


Figure 16a. Activity conc. at depth 24-32 cm with K-40

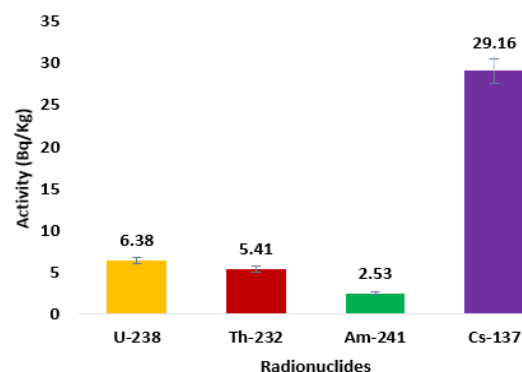


Figure 16b. Activity conc. at depth 24-32 cm without K-40

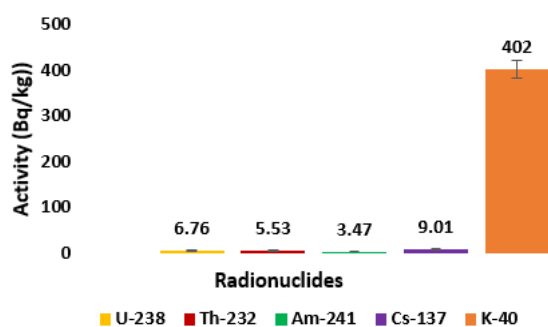


Figure 17a. Activity conc. at depth 32-40 cm with K-40

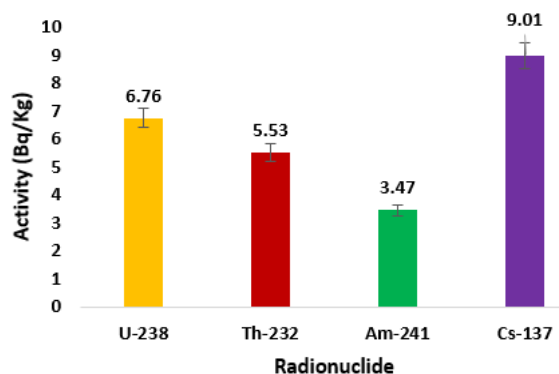


Figure 17b. Activity conc. at depth 32-40 cm without K-40

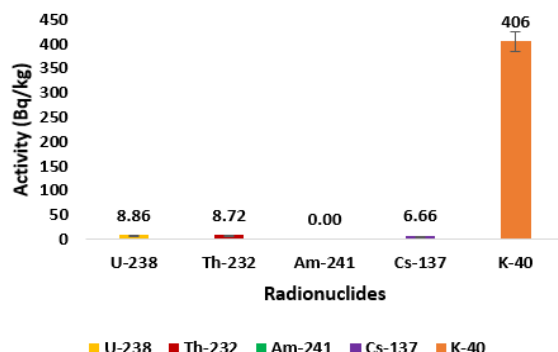


Figure 18a. Activity conc. at depth 40-48 cm with K-40

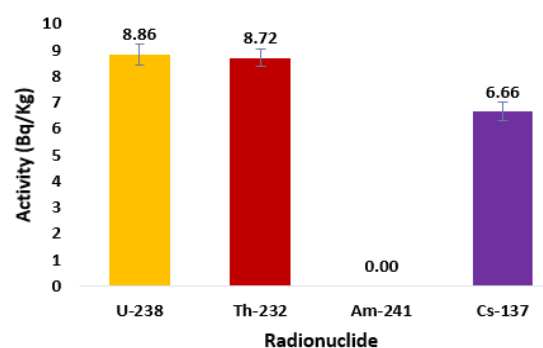


Figure 18b. Activity conc. at depth 40-48 cm without K-40

4. Results and Discussion

The experimental results of my investigation on the level of activity of isotopic radionuclides of U-238 and Th-232 used for the analysis at each depth; activity concentration with its uncertainty for U-238, Th-232, K-40, Cs-137 and Am-241 in each soil samples presented using both bar charts and line diagrams shown in figures (6, 7).

The measured sample soil activity concentrations of the natural radionuclides U-234, Th-232, and K-40, and the activity concentration of artificially produced radionuclide of Cs-137 and Am-241 of area of interest at West Kirby are shown in table 2 above. (BDL: 5.95 ± 0.32) Bq/kg and $(6.66 \pm 0.35 - 29.2 \pm 1.5)$ Bq/kg where BDL mean below detectable limit.

Figures (8, 9): Activity concentration levels of U-238 and Th-232 for topsoil sample at 0-5 cm to 40-48 cm depth. It was found that the slope of each trend line was slightly higher in the deeper soil samples than at the top soil. The activity concentration of U-238 is found to be varied from 5.37 ± 0.30 and 8.86 ± 0.40 Bq/kg and that of

Th-234 varied from 4.37 ± 0.31 and 8.72 ± 0.35 Bq/kg. For U-238 maximum and minimum activity concentration correspond to soil depths 40-48 cm and 0-8 cm respectively while maximum and minimum concentration for Th-234 correspond to depths 40-48 cm and 8-16 cm respectively. The mean activity concentrations of U-238 and Th-234 in the soil samples are 6.7 ± 0.1 Bq/kg and 5.6 ± 0.1 Bq/kg respectively.

K-40 activity concentration is much significant compared to the other radioactive nuclides as shown in figures (10-18). The K-40 activity concentration in the samples soil is found to varied from 384 ± 19 and 416 ± 21 Bq/kg. The maximum activity was found at the depth of 24-32 cm and minimum correspond to depth 0-8 cm. The mean activity concentration of K-40 in the sample soil is 398.2 ± 8.2 Bq/kg. The high concentration of K-40 which is an isotope of potassium is an important nutrient for plants available in abundance in soil is expected compared to other radionuclides. This high concentration value varies due to continuous uptake and accumulation of this radionuclides over a period of time.

Radioactive nuclides of anthropogenic Am-241 and Cs-137 released during the Chernobyl and Windscale, UK atmospheric testing and fallout of nuclear weapon accidents in nuclear facility detected worldwide in soil and sediments samples (NCRP, 1975), (Windscale, 1957). These are of high interest monitoring to protect and control the environment of contamination. From figures (10, 18), the soil activity concentrations of Am-241 ranged from below detectable limit (BDL) to 5.95 ± 0.32 Bq/kg in the soil. The maximum concentration was found on depth of 8-16 cm and BDL at depth 40-48 cm of soil that is Am-241 activity concentration was below minimum detectable activity. The mean activation concentration of Am-241 in the soil sample is 4.32 ± 0.11 Bq/kg.

The activity concentration of Cs-137, an anthropogenic nuclide in the soil samples value range from 6.66 ± 0.35 and 29.2 ± 1.5 Bq/kg respectively with mean activity concentration of 14.54 ± 0.34 Bq/kg as shown in figure (11). The maximum and minimum occur at depth of 24-32 cm and 40-48 cm respectively. The soil concentration variation of Cs-137 decrease significantly with depth due to fallout deposition. When Cs-137 reacts with soil by rainfall, it is absorbed and accumulated on small particles. Absorption by soils occurs mostly at the top of depth 24 cm.

5. Conclusions

The specific activities concentration for the soil samples under analysis is summarised in Table 2. Between the depth of interest of 0-48 cm, the average activity concentration of uranium-238, thorium-232, americium-241, cesium-137 and potassium-40 are 6.7 ± 0.1 Bq/kg, 5.6 ± 0.1 Bq/kg, 4.3 ± 0.1 Bq/kg, 14.5 ± 0.3 Bq/kg and 398.2 ± 8.2 Bq/kg respectively.

In comparison to the world average concentration of soil samples values of the natural radioactive nuclides U-238, Th-232 and K-40 are 40 Bq/kg, 37 Bq/kg and 370 Bq/kg respectively (UNSCEAR, 2000). Only potassium isotope has slightly mean activity concentration higher than the world average. My findings are in general agreement with the worldwide mean value.

The future work will be taking different soil samples from a nearby location to include various depths and analyse.

Also, a model of the identical geometry of soil samples is done using Monte Carlo simulation and compared the extent of contamination of the two results. Also, to work on the resolution of the 186 keV peak of Ra-226 due to the interference of 185.72 keV of U-235 and determine the U-235/U-238 isotopic ratio naturally.

References

- Abu-Haija, O. (2012). Determination of Natural Radionuclides Concentrations in Surface Soil in Tafila/Jordan. *Modern Applied Science*, 6(3). <https://doi.org/10.5539/mas.v6n3p87>
- Barba-Lobo, A., Gázquez, M. J., & Bolivar, J. P. (2022). A Practical Procedure to Determine Natural Radionuclides in Solid Materials from Mining. *Minerals*, 12(5), 611. <https://doi.org/10.3390/min12050611>
- Canberra. (2014). *Broad Energy Germanium Detectors (BEGe)*. Retrieved from <https://www.canberra.com/products/detectors/pdf/BEGe-SS-C40013.pdf>
- Canberra. (2014). *Lynx Digital Signal Analyzer*. Retrieved from https://www.canberra.com/products/radiochemistry_lab/pdf/Lynx-SS-C38658.pdf
- Doyle, C., & Povinec, P. P. (2004). *Quantification of Uncertainty in Gamma-spectrometric Analysis of Environmental Samples*.
- Gilmore, G. (2008). *Practical Gamma-Ray Spectroscopy* (2nd ed.). Chichester, West Sussex: J. Wiley & Son. <https://doi.org/10.1002/9780470861981>

- Guillen, J., Beresford, N. A., Baeza, A., Izquierdo, M., Wood, M. D., Salas, A., Munoz-Serrano, A., Corrales-Vazquez, J. M., & Munoz-Munoz, J. G. (2018). Transfer parameters for ICRP's Reference Animals and Plants in a terrestrial Mediterranean ecosystem. *Journal of Environmental Radioactivity*, 186, 9-22. <https://doi.org/10.1016/j.jenvrad.2017.06.024>
- Harkness-Brennana, L. J., Judson, D. S., Boston, A. J., Boston, H. C., Colosimo, S. J., Cresswell, J. R., . . . Mueller, W. F. (2014). An experimental characterisation of a Broad Energy Germanium detector. *Nuclear Instruments and Methods in Physics Research Section A: Accelerators, Spectrometers, Detectors and Associated Equipment*, 760, 28-39. <https://doi.org/10.1016/j.nima.2014.05.080>
- Jones, K. C., Stratford, J. A., Waterhouse, K. S., & Vogt, N. B. (1989). Organic contaminants in Welsh soils: Polynuclear aromatic hydrocarbons. *Environmental Science & Technology*, 23(5), 540-550. <https://doi.org/10.1021/es00063a005>
- Kathren, R. L. (1998). NORM Sources and their origins. *Applied radiation and isotopes*, 49(3), 149-168. [https://doi.org/10.1016/S0969-8043\(97\)00237-6](https://doi.org/10.1016/S0969-8043(97)00237-6)
- Knoll, G. F. (2010). *Radiation Detection and Measurement* (4th ed.). John Wiley and Sons, Inc.
- Lilley, J. (2001). *Nuclear Physics: Principle and Applications West Sussex*. John Wiley and Sons Ltd.
- National Council on Radiation Protection and Measurements. (NCRP). (1975). *Natural Background Radiation in the United States*. NCRP Report No. 45. Washington DC: NCRP.
- Thomas, R. L., Vernet, J. P., & Frank, R. (1984). ΣDDT, PCBs and HCB in the Sediments of Lake Geneva and the Upper Rhône River. *Environmental Geology*, 5, 103-113. <https://doi.org/10.1007/BF02381268>
- United Nations Sources and Effects of Ionizing Radiation. (2000). *Volume I: Sources; Volume II: Effects*. United Nations Scientific Committee on the Effects of Atomic Radiation, 2000 to the General Assembly, with scientific annexes. United Nations sales Publications E.00IX.3 and E.00.IX.4. United Nations, New York, 2000.
- Wolfgang, W. (2007). *Radionuclide handbook for laboratory workers*. Institute for Spectrometry and Radiation Protection. Windscale, UK. Retrieved from https://www.radioactivity.eu.com/site/pages/Windscale_Accident.htm
- Venhart, M., Wood, J. L., Boston, A. J., Cocolios, T. E., Harkness-Brennan, L. J., Herzberg, R. -D., . . . Veselsky, M. (2017). Application of the Broad Energy Germanium detector: A technique for elucidating beta-decay schemes which involve daughter nuclei with very low energy excited states. *Nuclear Instruments & Methods In Physics Research Section A: Accelerators Spectrometers Detectors And Associated Equipment*, 849, 112-118. <https://doi.org/10.1016/j.nima.2016.12.048>

Copyrights

Copyright for this article is retained by the author(s), with first publication rights granted to the journal.

This is an open-access article distributed under the terms and conditions of the Creative Commons Attribution license (<http://creativecommons.org/licenses/by/4.0/>).